

Electron in a Transverse Harmonic Cavity

H. Honkanen,^{1,*} P. Maris,^{1,†} J. P. Vary,^{1,‡} and S. J. Brodsky^{2,§}

¹*Department of Physics and Astronomy, Iowa State University, Ames, Iowa 50011, USA*

²*SLAC National Accelerator Laboratory, Stanford University, Menlo Park, California, USA*

(Received 31 July 2010; published 11 February 2011)

Recent experiments with heavy ions and planned experiments with ultraintense lasers require non-perturbative solutions to quantum field theory for predicting and interpreting the results. To propel this theoretical direction, we solve the nonperturbative problem of an electron in a strong transverse confining potential using Hamiltonian light-front quantum field theory. We evaluate both the invariant mass spectra and the anomalous magnetic moment of the lowest state for this two-scale system. The weak external field limit of the anomalous magnetic moment agrees with the result of QED perturbation theory within the anticipated accuracy.

DOI: [10.1103/PhysRevLett.106.061603](https://doi.org/10.1103/PhysRevLett.106.061603)

PACS numbers: 11.10.Ef, 11.15.Tk, 12.20.Ds

Recent intense interest in strong-field dynamics, ranging from the anomalous enhancement of lepton production in ultrarelativistic collisions between heavy nuclei at RHIC [1] and predicted photon yield depletion at the LHC [2], to proposals for producing supercritical fields with next-generation laser facilities [3,4], points to the importance of developing new methods for solving QED in its non-perturbative domain. An ideal tool for such problems is Hamiltonian light-front formalism [see, e.g., Ref. [5]], in which the gauge theory is quantized on the light front and the physical states are expanded in a Fock-space basis developed from the constituents. The Hamiltonian is represented as an operator acting on these Fock states. Since time is set along the light front, the ground state of the free theory is also a ground state of the full interacting theory and the formalism is Lorentz frame independent.

The light-front Hamiltonian approach provides a realization of Feynman's covariant "parton" model where the partons are the elementary fields used to define the Fock-space basis. It also has the appearance of a standard quantum many-body problem with the necessary quantum field theory features such as pair creation and annihilation. Diagonalization of the Hamiltonian provides amplitudes for evaluating experimental observables that are nonperturbative and relativistically invariant such as masses, form factors, and structure functions. The Fock-space dependence of observables is to be evaluated and one seeks to eliminate such dependence.

We address the problem of an electron in a transverse harmonic cavity and solve for its mass spectra and other observables as a function of the external field strength over a range spanning the electron mass. To accomplish this, we evaluate the QED Hamiltonian in light-front gauge on the light front in a Fock space consisting of electron states and electron plus photon states. We add the harmonic oscillator potential in the transverse direction to confine the system in those directions. We then solve for the eigenvalues, eigenvectors, and anomalous magnetic moment. The

nonperturbative analysis presented in this Letter could be applicable to measurements of the (gyromagnetic) ratio of the spin precession to Larmor frequencies of a trapped electron in strong external electromagnetic fields or intense time-dependent laser fields. This research also serves as a foundation for solving other quantum field theories at strong coupling, such as the light-front QCD Hamiltonian in the nonperturbative domain.

The question arises on how to implement a consistent renormalization program. Our specific choice is defined below. With our limits on the Fock space and adopted renormalization scheme, we can already demonstrate the effects of mass renormalization but not yet coupling constant renormalization. A full renormalization program will ensue when we enlarge our Fock-space basis to include electron-positron pairs. Such pairs produced at RHIC experience strong time-dependent electromagnetic fields. The total charge $Z_{\text{total}} = Z_1 + Z_2$ of the two colliding nuclei can exceed 137, indicating the need to treat the production and propagation properties with nonperturbative methods. In particular, the renormalization scale entering the running QED coupling is set by the photon virtuality which would be expected to be of order $Z_{\text{total}}\alpha\bar{m}_e$. The renormalization scale p^2 appearing in the electron running mass $\bar{m}(p^2)$ is of similar order. Such a full renormalization program will also allow comparison with higher order perturbative calculations such as those for an electron in a Penning trap [6].

We define our light-front coordinates as $x^\pm = x^0 \pm x^3$, $x^\perp = (x^1, x^2)$, where the variable x^+ is light-front time and x^- is the longitudinal coordinate. We adopt $x^+ = 0$, the "null plane," for our quantization surface. Here we adopt basis states for each constituent that consist of transverse 2D harmonic oscillator (HO) states combined with discretized longitudinal modes, plane waves, satisfying selected boundary conditions. This basis function approach follows [7] and is supported by successful anti-de Sitter-QCD models [8].

The HO states are characterized by a principal quantum number n , orbital quantum number m , and HO energy Ω . Working in momentum space, it is convenient to write the 2D oscillator as a function of the dimensionless variable $\rho = |p^\perp|/\sqrt{M_0\Omega}$, and M_0 has units of mass. The orthonormalized HO wave functions in polar coordinates (ρ, φ) are then given in terms of the generalized Laguerre polynomials, $L_n^{|m|}(\rho^2)$, by

$$\begin{aligned} \Phi_{nm}(\rho, \varphi) &= \langle \rho \varphi | nm \rangle \\ &= \sqrt{\frac{2\pi}{M_0\Omega}} \sqrt{\frac{2n!}{(|m|+n)!}} e^{im\varphi} \rho^{|m|} e^{-\rho^2/2} L_n^{|m|}(\rho^2), \end{aligned} \quad (1)$$

with eigenvalues $E_{n,m} = (2n + |m| + 1)\Omega$. The HO wave functions have the same analytic structure in both coordinate and momentum space, a feature reminiscent of a plane-wave basis.

The longitudinal modes, ψ_k , in our basis are defined for $-L \leq x^- \leq L$ with periodic boundary conditions for the photon and antiperiodic boundary conditions for the electron:

$$\psi_k(x^-) = \frac{1}{\sqrt{2L}} e^{i(\pi/L)kx^-}, \quad (2)$$

where $k = 1, 2, 3, \dots$ for periodic boundary conditions (we neglect the zero mode) and $k = \frac{1}{2}, \frac{3}{2}, \frac{5}{2}, \dots$ for antiperiodic boundary conditions. The full 3D single-particle basis state is defined by the product form

$$\Psi_{k,n,m}(x^-, \rho, \varphi) = \psi_k(x^-) \Phi_{n,m}(\rho, \varphi). \quad (3)$$

Following Ref. [5] we introduce the total invariant mass-squared M^2 for the low-lying physical states in terms of a Hamiltonian H times a dimensionless integer for the total light-front momentum K

$$M^2 + P_\perp P_\perp \rightarrow M^2 + \text{const} = P^+ P^- = KH \quad (4)$$

where we absorb the constant into M^2 . For simplicity, the transverse functions for both the electron and the photon are taken as eigenmodes of the trap. The noninteracting Hamiltonian $H_0 = 2M_0 P_c^-$ for this system is then defined by the sum of the occupied modes i in each many-parton state:

$$H_0 = \frac{2M_0\Omega}{K} \sum_i \frac{2n_i + |m_i| + 1 + \bar{m}_i^2/(2M_0\Omega)}{x_i}, \quad (5)$$

where \bar{m}_i is the mass of the parton i . The photon mass is set to zero throughout this work and the electron mass \bar{m}_e is set at the physical mass 0.511 MeV in our nonrenormalized calculations. We also set $M_0 = \bar{m}_e$.

The light-front QED Hamiltonian interaction terms we need are the electron to electron-photon vertex, given as

$$V_{e \rightarrow e\gamma} = g \int dx_+ d^2x_\perp \bar{\Psi}(x) \gamma^\mu \Psi(x) A_\mu(x) |_{x^+=0}, \quad (6)$$

and the instantaneous electron-photon interaction,

$$V_{e\gamma \rightarrow e\gamma} = \frac{g^2}{2} \int dx_+ d^2x_\perp \bar{\Psi} \gamma^\mu A_\mu \frac{\gamma^+}{i\partial^+} (\gamma^\nu A_\nu \Psi) |_{x^+=0}, \quad (7)$$

where the coupling constant $g^2 = 4\pi\alpha$, and α is the fine structure constant taken to be $\alpha = \frac{1}{137.036}$ in this work. The nonspinflip vertex terms of Eq. (6) are $\propto M_0\Omega$, whereas spinflip terms are $\propto \sqrt{M_0\Omega}m_e$. Selecting the initial state electron helicity in the single electron sector always as ‘‘up,’’ the process $e \rightarrow e\gamma$ is nonzero for three out of eight helicity combinations, and the process $e\gamma \rightarrow e\gamma$ is nonzero only with all four spin projections aligned (two out of 16 combinations), resulting in a sparse matrix.

We implement a symmetry constraint for the basis by fixing the total angular momentum projection $J_z = M + S = \frac{1}{2}$, where $M = \sum_i m_i$ is the total azimuthal quantum number, and $S = \sum_i s_i$ the total spin projection along the x^- direction. For cutoffs, we select the total light-front momentum, K , and the maximum total quanta allowed in the transverse mode of each one or two-parton state, N_{\max} , such that

$$\sum_i x_i = 1 = \frac{1}{K} \sum_i k_i, \quad (8)$$

$$\sum_i 2n_i + |m_i| + 1 \leq N_{\max}, \quad (9)$$

where, for example, k_i defines the longitudinal modes of Eq. (2) for the i th parton. Equation (8) signifies total light-front momentum conservation written in terms of boost-invariant momentum fractions, x_i . Since we employ a mix of boundary conditions and all states have half-integer total K , we will quote K values rounded downwards for convenience, except when the precise value is required.

In Fig. 1 we show the eigenvalues (multiplied by K) for a nonrenormalized light-front QED Hamiltonian given in

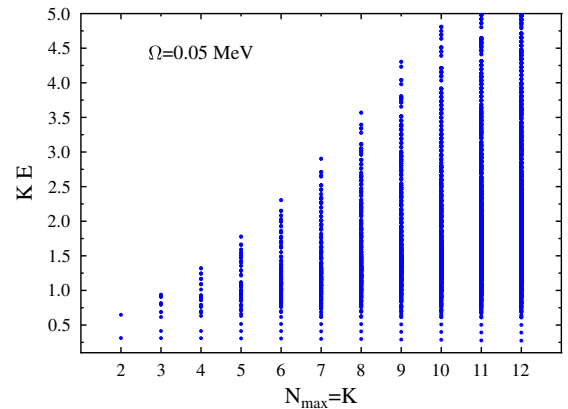


FIG. 1 (color online). Eigenvalues (multiplied by K) for a nonrenormalized light-front QED Hamiltonian which includes the electron-photon vertex and the instantaneous electron-photon interaction without counterterms. The cutoffs for the basis space dimensions are selected such that K increases simultaneously with the N_{\max} .

Eqs. (5)–(7), with fixed $\Omega = 0.05$ MeV and simultaneously increasing K and N_{\max} . The resulting dimension of the Hamiltonian matrix increases rapidly. For $N_{\max} = K = 2, 10,$ and 20 , the dimensions of the corresponding symmetric $d \times d$ matrices are $d = 2, 1670,$ and $26\,990$, respectively.

The number of the single electron basis states, considering all the symmetries, increases slowly with increasing $N_{\max} = K$ cutoff. For $N_{\max} = K = 2, 10,$ and 20 the number of single electron basis states is 1, 5, and 10, respectively. Our lowest-lying eigenvalue corresponds to a solution dominated by the electron with $n = m = 0$. The ordering of excited states, due to significant interaction mixing, does not always follow the highly degenerate unperturbed spectrum of Eq. (5). States dominated by spin-flipped electron-photon components are evident in the solutions. Nevertheless, the lowest-lying eigenvalues appear with nearly harmonic separations in Fig. 1 as would be expected at the coupling of QED. The multiplicity of the higher eigenstates increases rapidly with increasing $N_{\max} = K$ and the states exhibit stronger mixing with other states than the lowest-lying states. In principle, the electron-photon basis states interact directly with each other in leading order through the instantaneous electron-photon interaction, but numerically the effect of this interaction is very weak, and thus does not contribute significantly to the mixing. Even though we work within a Fock-space approach, our numerical results should approximate the lowest order perturbative QED results for sufficiently weak external field.

In Fig. 2 we show the results for the square root of the electron anomalous magnetic moment (scaled), $\sqrt{\delta\mu/g^2}$, as a function of Ω obtained from the lowest mass eigenstate. That is, we plot the magnitude of the probability amplitude that electron has its spin flipped relative to the single electron Fock-space component in the range where the results are converged. Since our system is in an external field, the lowest physical mass eigenstate (not known experimentally) can deviate from the free electron mass. Therefore, without renormalization, we only consider cases where the mass eigenvalue falls within 25% of the free electron mass. At zero external field we may compare our $\delta\mu$ to the QED one-loop contribution to the electron anomalous magnetic moment, the Schwinger result $\frac{\alpha}{2\pi}$ [9]. That is we compare our results with $\sqrt{\alpha/(2\pi g^2)} = \sqrt{1/8\pi^2}$. For even $N_{\max} = K$ the results converge rapidly for $N_{\max} = K \geq 14$. The results for odd cutoffs (not shown) track even cutoff results as $N_{\max} = K$ increases. Below $\Omega \lesssim 0.05$ MeV all interactions are quenched at fixed $N_{\max} = K$, and not converged, due in part to our requirement that the HO basis tracks the external field.

Figure 2 also shows an extrapolation of the above results for $N_{\max} = K = 12, \dots, 20$ to the zero external field limit $\Omega = 0$ MeV. We have only included the points above the peak at $\Omega \gtrsim 0.05$ MeV, where we have reasonable

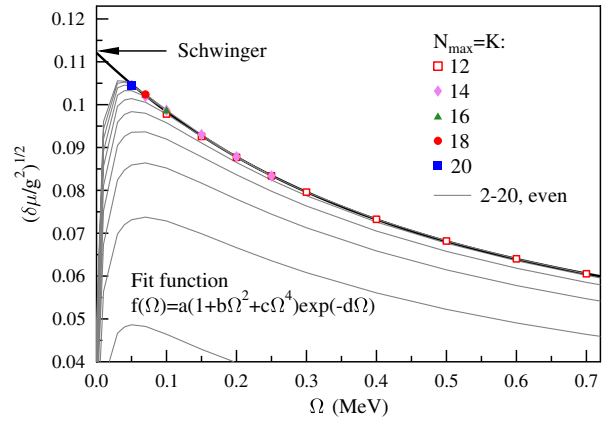


FIG. 2 (color online). Square root of the (scaled) electron anomalous magnetic moment as a function of the transverse external field for a sequence of increasing basis spaces (solid grey lines). These are nonrenormalized results where the mass eigenvalue falls within 25% of the free electron mass. The theoretical one-loop QED prediction (“Schwinger”) result of 0.1125, appropriate to $\Omega = 0$ MeV, is indicated. The black solid line is a fit to the results for $N_{\max} = K = 12, \dots, 20$, points included into the fit are indicated by the markers in the legend. Extrapolation to zero external field yields 0.1121.

convergence. An excellent agreement with the results is obtained by a fit function $f(\Omega) = a(1 + b\Omega^2 + c\Omega^4) \times \exp(-d\Omega)$, with $a = 0.1121$. This is $<1\%$ deviation from the Schwinger result of 0.1125, which is reasonable in light of our numerical accuracy and extrapolation uncertainties. If we perform individual extrapolations for all the $N_{\max} = K = 12, \dots, 20$ results with $0.1 \leq \Omega \leq 1.4$ MeV, a range spanning the electron mass scale, we obtain excellent fits with $0.1109 \leq a \leq 0.1134$, i.e., remaining within 1.5% of the Schwinger result.

In Ref. [7] we discussed possible divergences present in our framework, and anticipated a straightforward management of the identified divergences. Here we renormalize our results by applying a sector-dependent normalization scheme from Ref. [10]. In our present limited Fock space, we need only the mass counterterm δm_e . This δm_e is added to the mass term in the diagonal one-electron part of the Hamiltonian Eq. (5). In the absence of a known experimental mass for renormalization due to the external field, we adjust δm_e such that the lowest eigenstate remains at $KE_0 = m_e^2 + M_0\Omega$. That is, we simply adopt the free electron mass for the renormalized mass, and keep the coupling constant g^2 unchanged. We emphasize that our choice for the renormalized mass and for the coupling constant are, in principle, valid for the case of zero external field only. Measurements for electrons in a trap (see, e.g., [11]) could provide results leading to more precise renormalization parameters, but this aspect is beyond the scope of this Letter.

In Fig. 3 we present $\sqrt{\delta\mu/g^2}$ for $N_{\max} = K = 10, \dots, 20$ from the renormalized QED Hamiltonian of Eq. (5), with

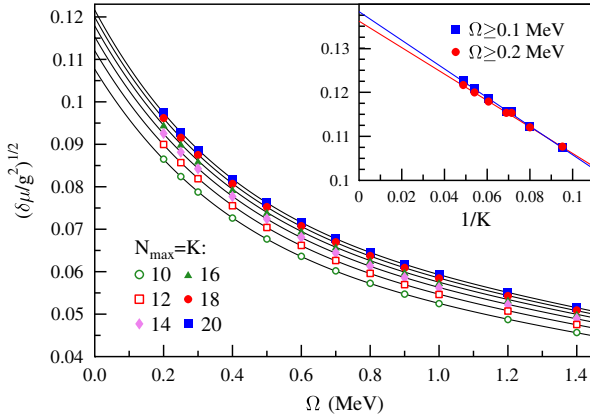


FIG. 3 (color online). Individual fits (solid black lines) to the renormalized results for square root of the (scaled) electron anomalous magnetic moment for $N_{\max} = K = 10, \dots, 20$. The inset shows the continuum limit extrapolation of the zero external field results in the main panel as a function of $1/K$.

δm_e , and Eqs. (6) and (7). To eliminate possible effects from the peak at $\Omega \sim 0.05$ MeV in Fig. 2, we only include results with the external field $\Omega \geq 0.2$ MeV. Again, individual fits of the form $f(\Omega) = a(1 + b\Omega^2 + c\Omega^4)\exp(-d\Omega)$ are an excellent representation of our results. The range of the extrapolated values is $0.1077 \leq a \leq 0.1216$.

The convergence with an increasing cutoff is now less rapid than in the nonrenormalized case shown in Fig. 2. In order to approach the continuum limit $N_{\max} = K \rightarrow \infty$, we perform further extrapolation to the zero- Ω results of Fig. 3. The inset of Fig. 3 shows linear extrapolation of the results of the main figure in $1/K$ to the continuum limit $N_{\max} = K \rightarrow \infty$. To verify the stability of the results, an extrapolation based on the $\Omega \geq 0.1$ MeV fits (not shown) is also given. The extrapolated continuum values are 0.1362 (0.1383) for $\Omega \geq 0.2(0.1)$, respectively, and thus about 20% above the Schwinger result 0.1125. An enhancement of this magnitude was also observed in related works, Refs. [12,13] and Refs. [14,15], where the one-photon truncated light-front Hamiltonian was regulated with Pauli-Villars regularization scheme. With Pauli-Villars regularization as well as in our renormalized results, interpreted from a perturbation theory perspective, the intermediate state propagators are developed from a dynamical (nonperturbative) electron mass rather than using the unperturbed mass needed for direct comparison with perturbation theory.

In our approach, the HO parameters Ω , M_0 , the electron mass m_e , and the total longitudinal momentum K appear as prefactors for the matrix elements in the Hamiltonian. Therefore, we can rather straightforwardly vary the size of the Hamiltonian matrix by keeping N_{\max} fixed, and changing K alone. We studied the continuum limit of $\sqrt{\delta\mu/g^2}$ by setting $N_{\max} = 20$ and increasing K in units of 10, from $K = 10$ to $K = 50$. The dimension of the Hamiltonian matrix then increases from $d = 11\,790$ to

$d = 69\,590$. The extrapolated results range between $0.1148 \leq a \leq 0.1259$, and show a good convergence pattern. Linear extrapolation of these results, analogously to Fig. 3, to the continuum limit $K \rightarrow \infty$ are 0.1288 (0.1290) with $\Omega \geq 0.2(0.1)$ MeV, $\sim 15\%$ above the Schwinger value.

In summary, we have evaluated properties of an electron in a nonperturbative external harmonic oscillator potential. We have taken the weak external field limit of the electron anomalous magnetic moment, and obtained results compatible with QED perturbation theory with reasonable accuracy. Our framework can be extended by incorporating higher Fock-space sectors and adopting external strong fields relevant to heavy ion collisions and to future high-intensity laser facilities. Applications to QCD will proceed with the adoption of recently developed color-singlet basis enumeration techniques [7].

The authors thank A. Harindranath, K. Tuchin, J. Hiller, S. Chabysheva, V. Karmanov, and A. Ilderton for fruitful discussions. Computational resources were provided by DOE through the National Energy Research Supercomputer Center (NERSC). This work was supported in part by a DOE Grant No. DE-FG02-87ER40371 and by DOE Contract No. DE-AC02-76SF00515.

*heli@iastate.edu

†pmaris@iastate.edu

‡jvary@iastate.edu

§sjbth@slac.stanford.edu

- [1] A. Adare *et al.* (PHENIX Collaboration), *Phys. Rev. C* **81**, 034911 (2010).
- [2] K. Tuchin, *arXiv:1008.1604*.
- [3] M. Ruf, G.R. Mocken, C. Muller, K.Z. Hatsagortsyan, and C.H. Keitel, *Phys. Rev. Lett.* **102**, 080402 (2009).
- [4] C.K. Dumlu and G.V. Dunne, *Phys. Rev. Lett.* **104**, 250402 (2010), and references therein.
- [5] S.J. Brodsky, H.C. Pauli, and S.S. Pinsky, *Phys. Rep.* **301**, 299 (1998).
- [6] L.S. Brown and G. Gabrielse, *Rev. Mod. Phys.* **58**, 233 (1986).
- [7] J.P. Vary *et al.*, *Phys. Rev. C* **81**, 035205 (2010).
- [8] G.F. de Teramond and S.J. Brodsky, *Phys. Rev. Lett.* **102**, 081601 (2009).
- [9] J.S. Schwinger, *Phys. Rev.* **73**, 416 (1948).
- [10] V.A. Karmanov, J.F. Mathiot, and A.V. Smirnov, *Phys. Rev. D* **77**, 085028 (2008).
- [11] D. Hanneke, S.F. Hoogerheide, and G. Gabrielse, *arXiv:1009.4831*.
- [12] S.J. Brodsky, J.R. Hiller, and G. McCartor, *Phys. Rev. D* **58**, 025005 (1998).
- [13] S.J. Brodsky, V.A. Franke, J.R. Hiller, G. McCartor, S.A. Paston, and E.V. Prokhvatilov, *Nucl. Phys.* **B703**, 333 (2004).
- [14] S.S. Chabysheva and J.R. Hiller, *Ann. Phys. (Leipzig)* **325**, 2435 (2010).
- [15] S.S. Chabysheva and J.R. Hiller, *Phys. Rev. D* **81**, 074030 (2010).